

# Palaeohydrology of the Seim River basin, Mid-Russian Upland, based on palaeochannel morphology and palynological data

Olga Borisova<sup>a</sup>, Aleksey Sidorchuk<sup>b,\*</sup>, Andrey Panin<sup>b</sup>

<sup>a</sup> *Institute of Geography, Russian Academy of Sciences, Staromonetny per., Moscow 109017, Russia*

<sup>b</sup> *Geographical Faculty, Moscow State University, Vorob'evy Gory, Moscow 119992, Russia*

Accepted 22 July 2005

## Abstract

Morphological, geological, geochronological and palynological analyses show that the landscape, climate and hydrological history of the Seim River basin includes: 1) a period of sandy Terrace 1 formation by shallow flows, with the surface transformation by cryogenic and aeolian processes, close to the Last Glaciation Maximum; 2) a cold and dry period about 16–14K radiocarbon years B.P. with very high surface runoff and extremely large meandering channel formation; 3) a period between the Oldest Dryas and the Preboreal of non-steady surface runoff decrease, large meander abandonment, and formation of smaller channels against the background of climate warming; 4) a period of relative stability of hydrological regime and small variations of water runoff as in modern rivers—throughout the Holocene.

© 2005 Elsevier B.V. All rights reserved.

*Keywords:* Holocene; Late Glacial; Palaeochannels; Palaeohydrology; Mid-Russian Upland

## 1. Introduction

The history of rivers and river valleys is a subject of palaeohydrology (the term first used by [Leopold and Miller, 1954](#)) originating from studies of fluvial morphology and alluvial chronology. Different approaches are used for palaeohydrological reconstructions, geomorphologic methods playing an important role ([Gregory, 1996](#)). Valuable information about hydrological regimes of the past can be derived from the morphology of former river channels and other features of the floodplain topography, especially when this former topography differs significantly from the present. More than a century ago [Davis \(1896\)](#) deduced that the small dimensions of contemporary meanders compared to the valley meanders suggested a significant reduction of the surface runoff, and proposed the term 'underfit rivers'. In the 1960s, interest in palaeochannel morphology and palaeohydrological reconstructions was

stimulated by classic studies by [Dury \(1958, 1964a,b, 1965\)](#), who showed a wide geographic occurrence of large meandering palaeochannels and argued for a dramatic decline of river discharges in temperate latitudes of North America, West and Central Europe at the termination of the Last Glacial epoch. At the same time [Volkov \(1960, 1962, 1963\)](#) studied palaeochannels on low river terraces in the southern West Siberia and obtained similar results.

The last four decades of the 20th century saw a significant development in morphological and sedimentological studies of past river behaviour in changeable environments (see, for example, palaeohydrological bibliography on the GLOCOPH web page at <http://www.ccma.csic.es/dpts/suelos/hidro/glocoph/home.html>). Recent studies provided comprehensive information about palaeochannel morphology on the Russian Plain ([Panin et al., 1999, 2001; Sidorchuk et al., 2001a,b](#)), allowing the identification of a circumpolar belt in the Northern Hemisphere, marked by dramatic changes in surface runoff during the last 14–16Kyr B.P. ([Sidorchuk, 2003](#)). About 70 sites with well-preserved remnants of large palaeochannels on the low terraces and floodplains have been detected over the

\* Corresponding author.

E-mail address: [yas@yas.geogr.msu.su](mailto:yas@yas.geogr.msu.su) (A. Sidorchuk).

Russian Plain (Sidorchuk et al., 2001a). Among them, one of the most interesting is the Seim River basin. This paper is aimed at (1) analysis of the palaeoenvironmental conditions and causes for the palaeohydrological changes, and (2) palaeohydrological reconstruction in the Seim River basin since the Late Pleniglacial.

## 2. The Seim River basin

The Seim River system drains the western slope of the Mid-Russian Upland into the Desna River, middle Dnepr basin (Fig. 1). The terrain is a dissected upland with the watersheds up to 230–280 m a.s.l., a dense erosion network and typical relief of nearly 100 m. The Seim River valley in its middle course generally follows the boundary of deciduous forest and forest steppe zones. Climate is temperate continental. Mean January and July temperatures are  $-8$  and  $+19^{\circ}\text{C}$ , respectively, annual precipitation varies over the basin in the range 475–625 mm. Annual discharge of the Seim River near L'gov (basin area  $10,700\text{ km}^2$ ) is  $42.4\text{ m}^3\text{ s}^{-1}$  (runoff depth 125 mm), that of the Svapa River near the mouth (basin area  $6310\text{ km}^2$ ) is  $23.0\text{ m}^3\text{ s}^{-1}$  (runoff depth 115 mm). About 70% of the precipitation falls during

the warm period (April–October), but the rivers are mainly snowmelt fed. The 1.5–2 months (April–May) of spring flood are the time when the most work on channel transformation is carried out. Mean flood discharge of the Seim River near L'gov is  $745\text{ m}^3\text{ s}^{-1}$ , and that of the Svapa River near mouth is  $442\text{ m}^3\text{ s}^{-1}$ . The rest of the year is characterised by low water which may be interrupted by 2–3 relatively minor short rainstorm floods in summer and autumn. The rivers are ice-covered from the end of November until March.

During its Quaternary history, glacial activity in the region only occurred in the Middle Pleistocene during the maximum stage of the Dnepr Glaciation (an analogue of the Saale Glaciation, OIS 6—according to Velichko et al., 2001), when the ice sheet occupied only the lower reaches of the Seim River basin (Fig. 1). In the Late Quaternary, the southern limit of the ice-sheet stretched about 500 km north of the Seim River valley; so that neither a damming effect, nor the glacial melt water influenced the development of the river.

River valleys in the Seim basin are rather wide and 80–100 m deep. Khrutskiy (1983) detected four major terrace levels. The heights of alluvial terraces are given with respect to the summer low water level (LWL), if no alternative indication is specified. In the lower Seim valley the 4–

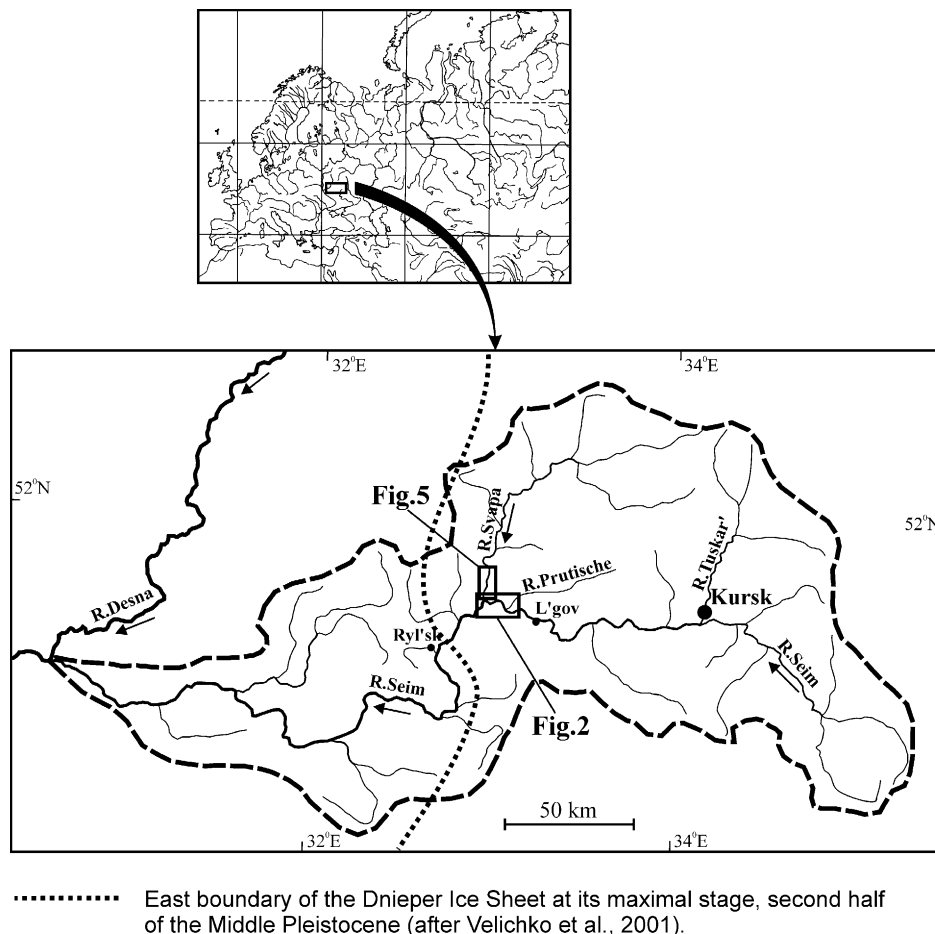


Fig. 1. Location of the Seim River basin and the key sites.

15 km wide and 50–60 m high Terrace IV is covered by the Dnepr (Saale) moraine, this indicates its pre-Dnepr age. Terrace III (30–40 m high) is correlated with the final (Moscow) stage of the Dnepr Glaciation, corresponding to the final part of the Middle Pleistocene. Terrace II (1–3 km wide and 16–24 m high) is found mostly on the left side of the Seim valley. This terrace corresponds to the 20–25 m terrace of the middle Desna River formed during the Early Valdai (Early Weichselian) glacial epoch, OIS 4 (Velichko et al., 1997). Terrace I (8–12 m) is found everywhere, its width varying from 200–300 m to 4–8 km. It was formed during the Late Valdai (Late Weichselian) glacial epoch (Khrutskiy, 1983).

### 3. Methods

#### 3.1. Alluvial features: morphology and geology

Palaeochannels and alluvial units in the 25 km section of the Seim valley downstream from L'gov (Fig. 2) and the 15 km section of Svapa valley at the river mouth (Fig. 3) were studied with the use of space images of 5–15 m resolution. A topographic survey of the key sites was made using GPS device Trimble 4000 SSE/SST with 10 cm accuracy.

In the field, the geological composition of palaeochannel infill, channel and overbank deposits on the floodplain and river terraces were studied both in natural exposures and by coring. Samples were collected with 2 cm resolution in the outcrops and 10 cm resolution in the cores. The age of alluvial deposits was determined by conventional radiocarbon dating of the organic matter. The date of active channel development corresponds to the age of channel alluvium. As these sediments are usually devoid of organic matter, the dates were mainly obtained on the infill of palaeochannels. Such dates are necessarily younger than the date of channel activity, but those obtained from the very base of the infill should be close to the moment of the palaeochannel abandonment and are considered to represent the upper limit of the palaeochannel development. If not specially designated, the age of sediments and events in the text is given in non-calibrated radiocarbon time. Pollen analyses were performed for the dated core and for the majority of dated samples from other sections. Morphological and geological data were further used for palaeohydrological and palaeogeographical reconstructions.

#### 3.2. Methods of palaeodischarge estimation

There are two main ways of calculating palaeodischarges with river channel morphology and texture: using either hydraulic or regime equations, both first used by Dury (1965).

The hydraulic approach requires detailed field investigations. The longitudinal profile and cross-section morphology of each channel, as well as the texture of the

infilling sediment must be carefully studied (Rotnicki and Borowka, 1985). Cross-sections at the riffles (crosses) of the meandering palaeochannels are the best for the reconstruction of water discharge  $Q$  ( $\text{m}^3 \text{s}^{-1}$ ). The Chezy–Manning formula can be used in calculations:

$$Q = A \frac{D^{1/6}}{n} \sqrt{SD} \quad (1)$$

The bottom of a palaeochannel corresponds to the top of the basal layer of coarse alluvium, which usually is exposed at the channel bed during extreme floods. The cross-section area  $A$  ( $\text{m}^2$ ) and its mean depth  $D$  (m) can be calculated for different water stages. The slope  $S$  is presumably stage-independent and equal to the longitudinal slope of the mean surface of the infilling deposits, but in reality it varies over time as do terrace gradients. The Manning roughness coefficient  $n$  ( $\text{s m}^{-1/3}$ ) can be estimated from the modern fluvial analogue of the palaeochannel. A lifetime of the palaeochannel and the return period of the extreme discharge are calculated using the meander evolution model. Mean maximum and annual discharges with different return periods can be calculated with the use of the two-parametric gamma-distribution and Gudrich distribution, the distribution parameters being obtained from modern fluvial analogues (for details see Sidorchuk and Borisova, 2000).

In the regime equations approach the relationships between channel morphology and flow hydrology are used. In this investigation, relationships between the mean annual discharge ( $Q_a$ ) and the bankfull channel width ( $W_b$ ) were established for meandering rivers in the Russian Plain, West and East Siberia:

$$Q_a = 0.012y^{0.73} W_b^{1.36} \quad (2)$$

The parameter  $y$  is in inverse relation to the seasonal flow variability and represents the ratio between the annual discharge  $Q_a$  and the mean maximum discharge  $Q_{\max}$ :

$$y = 100 (Q_a/Q_{\max}) \quad (3)$$

An increase in the flow variability (a decrease of  $y$ ) generally causes an increase in the floodplain height and flow concentration in a single channel with larger bankfull width. Flow variability depends on the basin area  $F$  ( $\text{km}^2$ ):

$$y = aF^{0.125} \quad (4)$$

Parameter  $a$  in formula (4) reflects the geographical distribution of the flow variability and can be estimated for each palaeochannel using recent fluvial analogues. Then it is possible to calculate  $y$  with formula (4), the mean annual discharge  $Q_a$  from the palaeochannel width with formula (2), and the mean maximum discharge  $Q_{\max}$  with formula (3).

#### 3.3. Principle of palaeogeographical analogy

To use both methods of palaeohydrological reconstruction, it is crucial to determine the recent region-analogue

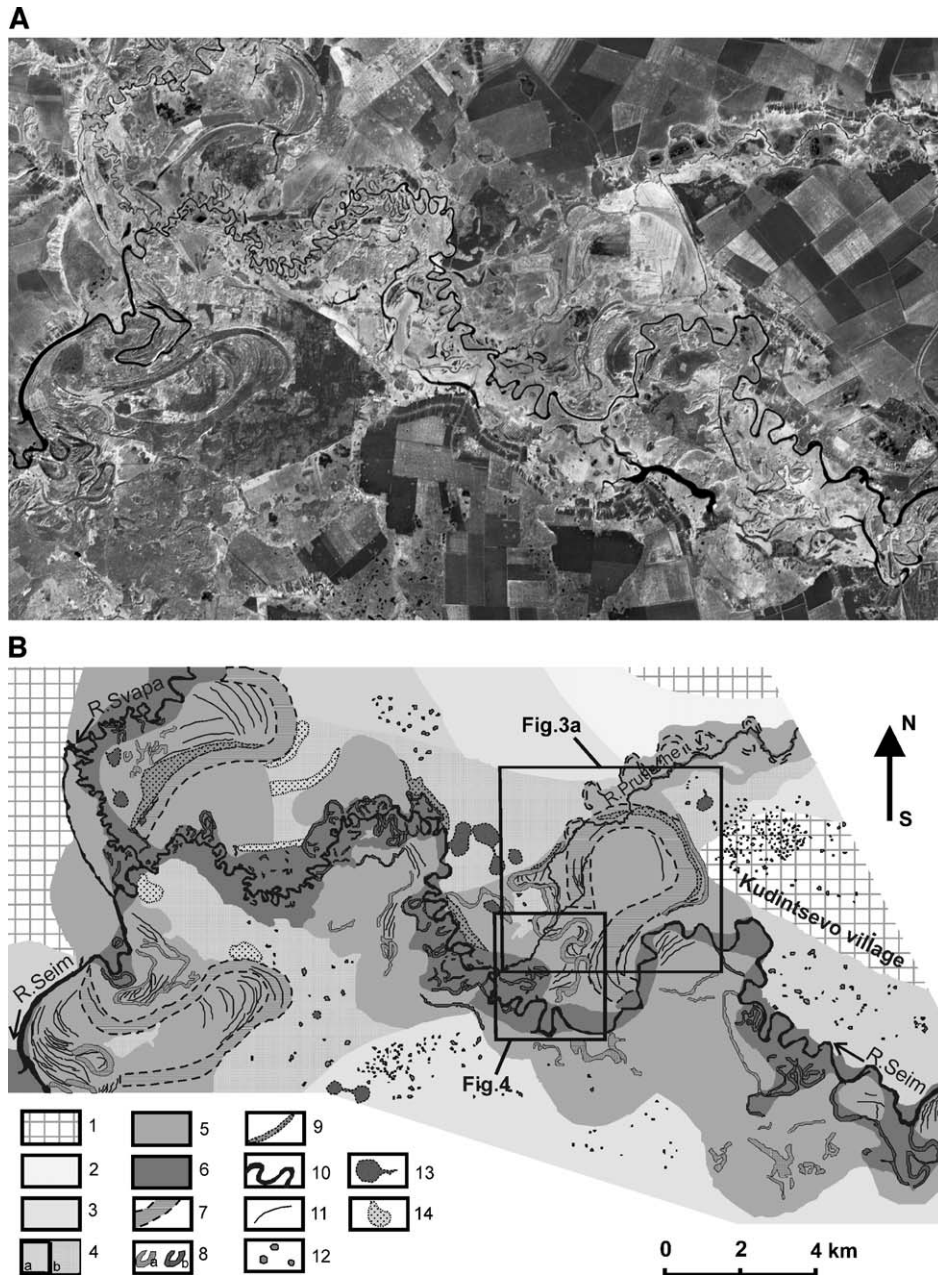


Fig. 2. The Seim River downstream from the L'gov town: a 15 m resolution space image (A) and geomorphological map (B). See location in Fig. 1. Legend: 1—watersheds and valley boundaries. Alluvial surfaces of various age: 2—Terrace II (18–25 m); 3—Terrace Ib (12–15 m); 4—Terrace Ia (a—Ia2, b—Ia1); 5—Late Glacial floodplain; 6—Holocene floodplain. Fluvial forms: 7—large palaeomeanders; 8—small ox-bows (a—Late Glacial, b—Holocene); 9—present channel; 10—big alluvial ridges; 11—floodplain levees. Relic non-fluvial forms: 12—“steppe dishes”; 13—thermokarst depressions (alases); 14—large aeolian hills and ridges.

and the fluvial analogue (Sidorchuk and Borisova, 2000). Geographical influences on river flow bring about similarity of hydrological regimes for rivers in similar landscapes (Evstigneev, 1990). Geographical controls over river flow and their applications to palaeohydrology lead to the principle of palaeogeographical analogy:

- a hydrological regime of a palaeoriver within a palaeolandscape must have been similar to that of a present-day river within the same type of landscape.

Therefore, for a palaeohydrological reconstruction the reconstruction of the palaeolandscape is required. The hydrological regime of modern rivers in a certain type of landscape can be used for estimations of the palaeohydrological regime in the same type of palaeolandscape.

To reconstruct the landscape and climatic conditions that existed at various stages of palaeochannel development, palynological studies of dated alluvium, lake and peat sediments, were performed. The use of palaeobotanic data for palaeoclimatic and palaeolandscape reconstruction



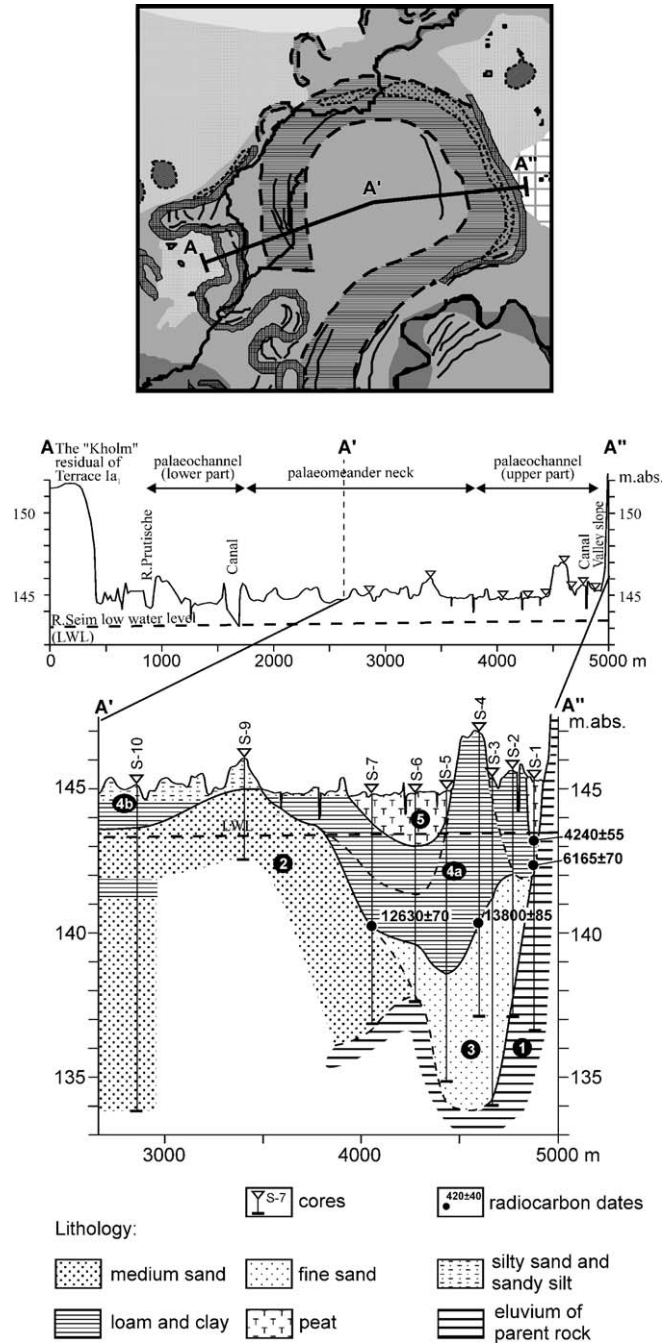


Fig. 3. Topographic and geological sections across the large meandering channel of Palaeo-Seim River near Kudintsevo village. See Fig. 2 for location. Circled numbers are stratigraphical units (as in the text).

implies that the flora of a particular region directly reflects the influence of the natural environment and of the climate in particular. Geographical analysis of the modern spatial distribution of all the plants of a certain fossil flora allows finding the location of the closest modern floristic analogue to the past vegetation at the site. By identifying the region where the majority of plant species found in a fossil flora are growing at the present time, it is possible to determine the closest modern landscape and climatic analogue of the past environment under consideration (Grichuk, 1969). Usually

the conditions suitable for all the species of a given fossil flora can be found within a comparatively small area. The present-day features of plant communities and the main climatic indices of such a region-analogue would be close, in most cases, if not identical, to those that existed at the site in the past.

Palynological analyses of 31 samples from section SV-8 were performed. Most samples from this section are relatively rich in pollen, its preservation being the best in the organic deposits. The pollen counting (200–300 pollen

grains per sample for eight samples and 300–500 grains per sample for the rest of the profile) was saved as TILIA file. Pollen diagrams based on the tree pollen sum and non-arboreal pollen sum were drawn, using TiliaGraph 1.20 (Grimm, 1990). This way of separate calculations for arboreal and non-arboreal components, traditionally used in Russian literature, was applied in an attempt to distinguish the specific changes in the composition of the woodlands and open plant communities (Fig. 9a,b). Zonation of the diagrams was made using CONISS program (Grimm, 1987). The local pollen assemblage zones (LPAZ) were then correlated to the European biostratigraphic Blytt–Sernander zones, slightly modified for northern Eurasia by Khotinsky (1977).

Seven radiocarbon-dated pollen assemblages, characteristic for each main LPAZ were studied in more detail to investigate the composition of the fossil floras. An attempt was made to achieve the highest possible taxonomic resolution, pollen identifications being made to species or genus levels for arboreal plants and for certain groups of herbaceous plants. In some cases, the floristic lists for two or three successive samples were combined to obtain more complete resulting lists of fossil floras. This was possible only in the case of close resemblance between pollen spectra of successive samples.

In addition to the pollen profile from SV-8 core, detail pollen analyses of seven samples from other sections of fluvial deposits, filling in the palaeochannels in the adjacent parts of the Seim River basin, were performed. These data were compared with those on section SV-8. The floristic lists compiled for five of these samples were used along with seven fossil floras from section SV-8 to reconstruct the main landscape and climatic changes in the region during the Late Glacial and the Holocene.

#### 4. Morphology and geology of the Seim River valley downstream from L'gov

##### 4.1. Low terraces

In the valley of the Seim River at L'gov town, Terrace I occupies a wider elevation range than detected by Khrutskiy (1983) and is split into two sub-levels (Panin et al., 2001): Terrace Ia 7–10m high and Terrace Ib 12–15m high. Terrace Ia is represented by two morphological units (Fig. 2B). Unit Ia<sub>2</sub> is characterised by more flat topography with channel sands covered by loam 3–4m thick (overbank alluvium). Unit Ia<sub>1</sub>, widely spread in the Seim valley, is of relatively high relief due to a subsequent reworking of the initial alluvial surface by aeolian, thermokarst and fluvial processes. Loam cover here is thin or even absent, and channel sands are exposed at the surface promoting aeolian activity. The largest aeolian features are rounded sand hills up to 1km wide, rising 5–7m above the surface of the terrace (Fig. 2B). As everywhere, small so-called steppe

dishes of oval and round shape 20 to 100m in diameter are abundant on this terrace, along with the deep isometric depressions 250–700m wide with the bottoms lying only 3–4m above LWL. A peculiar morphological feature of these depressions is the 'flow-off' channels indicating the outbursts of former lakes. These features are interpreted as 'alas' (thermokarst) depressions formed due to the thaw of the ice-wedges on the floodplain in the Late Valdai. Terrace Ia<sub>1</sub> is also covered by a dendrite net of elongated depressions (channels). These channels could be formed as the result of erosion by the overbank flow during floods, which followed the chains of thermokarst depressions on the floodplain. Such processes are common in the Subarctic river valleys at present (Sidorchuk, 1975). The bottoms of these channels are only 3–5m above LWL, so that they can be occasionally inundated during modern floods. Fragments of the initial 7–10m terrace with steppe dishes, isolated by erosion processes, are preserved between elongated depressions, such as, for example, the one near the Kholm village (Fig. 2B).

##### 4.2. Pre-Holocene floodplain

Two main steps of the old (pre-Holocene) floodplain were formed on the Seim River and its main tributaries. The first is 4–6m high with a flat surface, its remnants being situated mainly along the sides of the valley bottom. It is rarely flooded at the present time, and several permanent settlements are located here.

The second step of the floodplain is characterised by a sequence of arcs with the radii of curvature exceeding that of the modern river channel bends by an order of magnitude (Fig. 2). Systems of natural levees and large abandoned oxbows are well defined on the air photographs. Systems of levees and hollows with the relative relief of 0.5–1.5m indicate steeply curved meandering palaeochannels with the wavelength 3.3–6.5km and the width 350–700m. This floodplain step with the remains of large palaeochannels lies largely at 2.0–2.5m above LWL and usually gets inundated during floods. Only the tops of the highest levees are as high as 3–3.5m and can be above the flood level.

##### 4.3. Large meanders

The large palaeochannel of the Seim River (Figs. 2, 3) formed highly curved meanders with the mean wavelength of 5400m and the mean length along the channel 14,000m. The mean shape coefficient is 2.6. Such an omega-like meander shape, with the shape coefficient considerably exceeding the optimum value for a meandering channel (which is 1.6 after Makkaveev, 1955), could have resulted either from low flooding levels or from high stability of the floodplain. The palaeochannel section near the Kudintsevo village represents a large loop, slightly recumbent up the valley, with the meander amplitude of 4km and the half-wavelength of 3km. The palaeomeander neck near the Krasnaya Zarya village is

very narrow, so that the systems of natural levees and troughs on the upper and lower sides of this large bend nearly come into contact there (see Figs. 2, 3).

The texture of this large palaeochannel infilling was investigated by coring along the profile A'–A'' in the upper part of the bend (Fig. 3). The palaeochannel cross-section has an asymmetrical triangular shape. Its deepest part (6–6.5 m, app. 10 m below LWL) is shifted towards the steep concave bank of the palaeomeander. Several boreholes (S-2, S-3, and S-6) reached the deposits underlying the channel alluvium (unit 1). They are represented by poorly sorted sandy loam with a uniform distribution of all fractions, from clay to coarse sand. These sediments contain secondary sulphides in the form of small concretions and pellicles (more than 47% of heavy minerals in the fine sand fraction). A long period of diagenesis in submerged (lacustrine or marine) conditions was necessary for their formation. As these sediments contain also the microfossils of presumably Cretaceous age (Hystrichosphaeridae), they probably represent an eluvium of the Cretaceous bedrocks. The opposite gently sloping bank of the palaeochannel is formed by system of broad point bars, composed of medium-grained sand (borehole S-7), similar to the sand in the meander neck (unit 2, boreholes S-9, S-10).

The palaeochannel fill includes three main units. The lowermost unit 3 is fine silt sand 5–7 m thick. It may be interpreted in two ways. First, this sand may represent channel alluvium of the late stages of the active meander development. In this case the bottom of the palaeochannel

corresponds to the roof of this sand. The alternative is that these deposits represent channel silting which started immediately after the meander abandonment. In this case the palaeochannel bottom corresponds to the base of unit 3. As the amplitudes of seasonal deformations on sandy rivers are very high, it is impossible to determine the exact position of an ancient riverbed exclusively on the basis of the geological data. On the Russian Plain pools on big rivers are typically deepening during floods and aggrading during the periods of low water by 0.5–1.0 m (Makkaveev, 1955).

The sand is overlain by grey clay and silt accumulated largely in the oxbow lake on the floodplain (unit 4a). Near their base, these deposits are generally sandy and contain thin layers of sand. In the upper part they contain more clay, as the oxbow lake gradually became more isolated. The deposits at the base of unit 4a were radiocarbon-dated based on the bulk organic matter to 12,630±70 and 13,800±85 years B.P (samples Ki-6985 and Ki-6984). We assume that the latter date indicates the time shortly after the macromeander was abandoned. While the palaeochannel was filling in, the over-bank sedimentation on the floodplain continued (unit 4b).

In the process of accumulation of the oxbow clays a 4 km long in-channel levee had been formed (Figs. 2B, 3). This levee extends along the upstream side of the palaeomeander and consists of the same clays as the rest of unit 4a. Its flat top 200 m wide lies at 3.5 m above LWL and is not subjected to flooding, as indicated by the grey forest soil (Greyzem). Probably the levee was formed as the result of high floods at the time when the meander had already been abandoned but

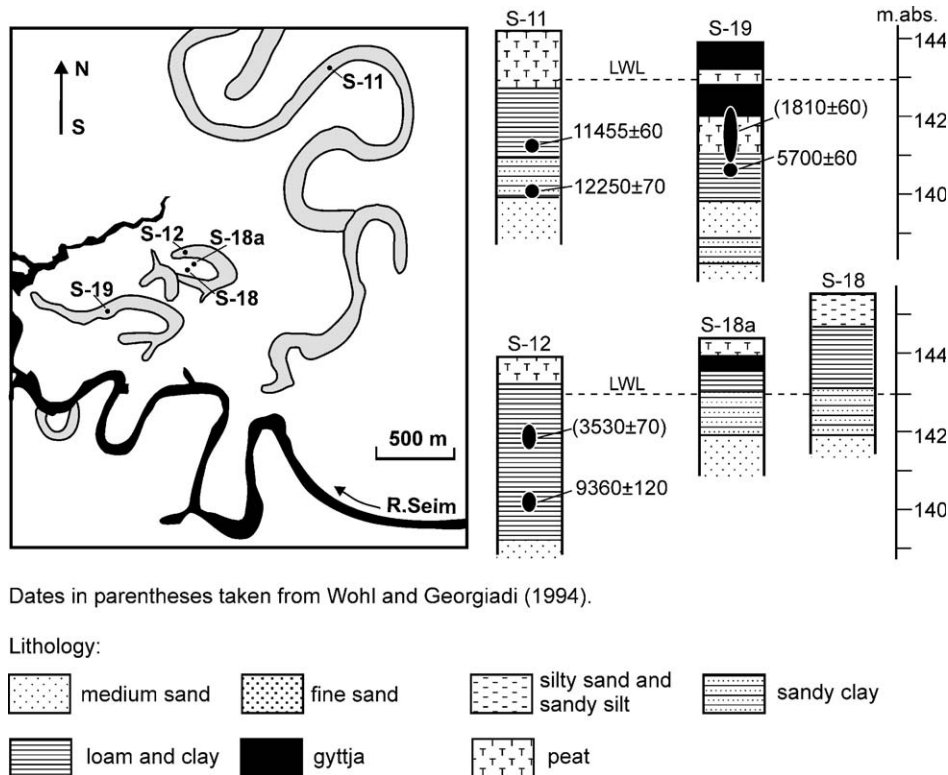


Fig. 4. Secondary meandering channel and small ox-bows of the Seim River near Kudintsevo village. See Fig. 2 for location.



still represented a well-shaped depression concentrating the flood flows. Low organic matter content in the clays may indicate the pre-Holocene age of the levee, its top therefore providing a minimal estimation of the flood levels in the Late Glacial. The levee has divided the palaeochannel into two hollows, which aggraded separately. By the beginning of the Holocene the palaeochannel had been filled up to the river LWL. The oxbow lake transformed into a fen, and mineral deposition changed to peat accumulation (unit 5). By 1950th, when a net of artificial ditches and canals drained the floodplain, the thickness of the peat layer reached 2 m, or 1.4–1.5 m above LWL.

Several natural levees and troughs are preserved on the neck of the palaeomeander. These levees are 100–200 m wide and 2.5–3.0 m high above the LWL. They consist of sandy clay within the top meter and of channel alluvial sand below it. Within its oldest part, the surface of the palaeomeander neck lies at 3.5–4 m above the LWL, so that at present it is not flooded. The difference of altitude between the palaeochannel pool and the tops of the levees (that is, the estimated Late Valdai flood level) is 14 m.

In the lower part of the large palaeomeander of the Seim River, a secondary meandering channel with the width of

100 m and the wavelength of 1300 m can be seen (Fig. 4). Its bends are omega-shaped and arc-shaped. There are well-developed series of natural levees and troughs at the necks of meanders. This palaeochannel was abandoned and filled in with clayey sediments not later than 12,300 years B.P. ( $^{14}\text{C}$  dates  $12,250 \pm 70$ , Ki-6987 and  $11,455 \pm 60$ , Ki-6986). Within the Seim River floodplain downstream from the large meander near Kudintsevo village, there are fragments of palaeochannels, similar in their widths and meander wavelengths to the above-mentioned secondary palaeochannel.

#### 4.4. The Holocene ox-bows

The Holocene ox-bows have meander size and width within the variability of present channel meanders of the Seim River (Fig. 4). Their fill consists of sandy loams or clays 2–3 m thick overlain by 0.5–1.5 m of peat with the black clay at the base. At the depth of 3–5 m fine- to medium-grained channel sands are found. Radiocarbon dating of the lower parts of the infill (see Fig. 4) indicates that these meanders became abandoned in the early and middle Holocene. These dates correspond well to the ages, published by Wohl and Georgiadi (1994), who studied the same ox-bows.

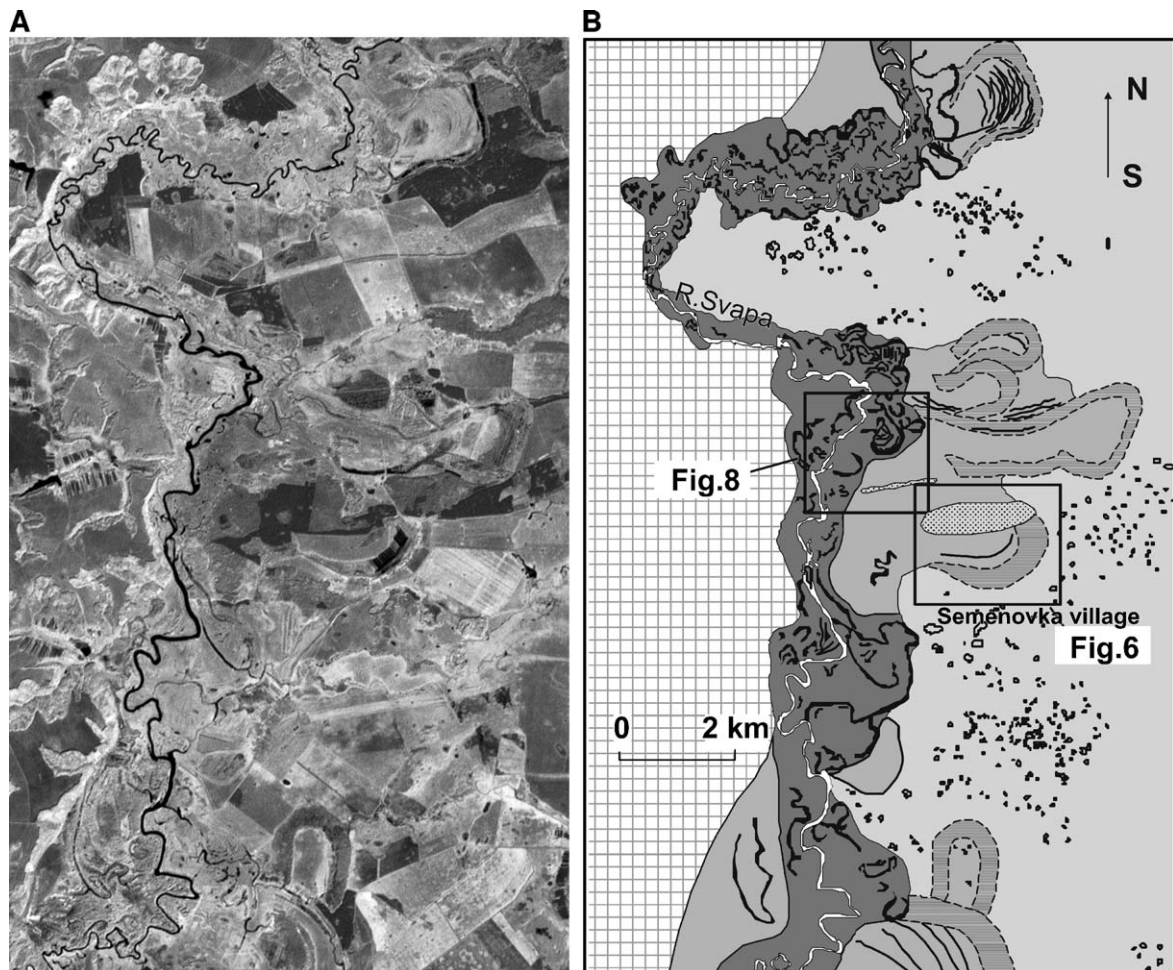


Fig. 5. The lower Svapa River: 15 m resolution space image (A) and geomorphological map (B). See Fig. 1 for location and Fig. 2 for legend.



## 5. Morphology and geology of the lower Svapa River

### 5.1. Low terrace—the Late Pleniglacial floodplain

In the Svapa River valley (Fig. 5) the 7–10 m terrace is represented by morphological unit Ia<sub>2</sub> with a relatively flat sub-horizontal surface. Original fluvial features can hardly be traced on the surface of this terrace. In places, there are series of narrow elongated depressions, partly inherited by shallow valleys of modern streams, separated by low levees. The primary fluvial relief of the terrace was partly masked by subsequent accumulation of fine-grained sediments. Its surface is covered by numerous small depressions (so-called “steppe dishes”), which are relic cryogenic micro-relief forms. These depressions have elongated or almost round shapes with the diameters ranging from 20–30 to 80–100 m.

### 5.2. Large meanders

In the Svapa River valley, the palaeochannel formed steeply curved meanders with the mean wavelength  $L$  of 2800 m and the mean length along the channel  $S$  of 3800 m (Figs. 5, 6). The mean shape coefficient ( $S/L$ ) for such meanders is 2.8, though it reaches 11 for the most sharply curved (finger-shaped or goose-neck) meanders. In that case, the coefficient exceeds considerably the optimum value for a meandering channel. A high resistance of the floodplain sediments to erosion can explain this discrepancy. Numerous

traces of palaeocryogenic microrelief can be seen on the surface of the Late Valdai floodplain (a contemporary terrace with the height of 7–10 m above LWL). Accordingly, the high erosional stability of the floodplain in the Late Valdai can be attributed to permafrost existence at that time. Contemporary rivers in the Yamal Peninsula can be considered an analogue to the palaeo-Svapa river during the stage of development of the large meanders, as they form sharp meanders within wide floodplains with sediments cemented by permafrost (see, Sidorchuk, 1996).

The palaeochannel in the Svapa River valley near Semenovka village is clearly expressed in the modern topography (Figs. 5, 6). Its bottom lies only 4 m above the modern LWL, so that it is submerged during high floods. The coring shows a box-shaped profile of the channel trough. The top surface of the fine- and medium-grained channel alluvial sands (an analogue of unit 3 in the Seim River palaeochannel infill) lies 1.5–2.5 m below the modern LWL. Silt and clay deposits with lenses of clayey sand (unit 4) fill in the trough. The accumulation of the fine-grained sediments began due to abandonment of the palaeochannel in the Oldest Dryas, not later than 14 Kyr B.P. (14,030 ± 70 years B.P., Ki-6997) and continued during the Bølling and the Allerød (12,360 ± 110, Ki-6999 and 11,755 ± 80, Ki-6996). In the end of the Late Glacial—beginning of the Holocene the palaeochannel almost entirely dried up, and the rate of deposition became very low. Peat formation (unit 5) started in the late Preboreal (9120 ± 70, Ki-6995; 9300 ± 120, GIN-11951).

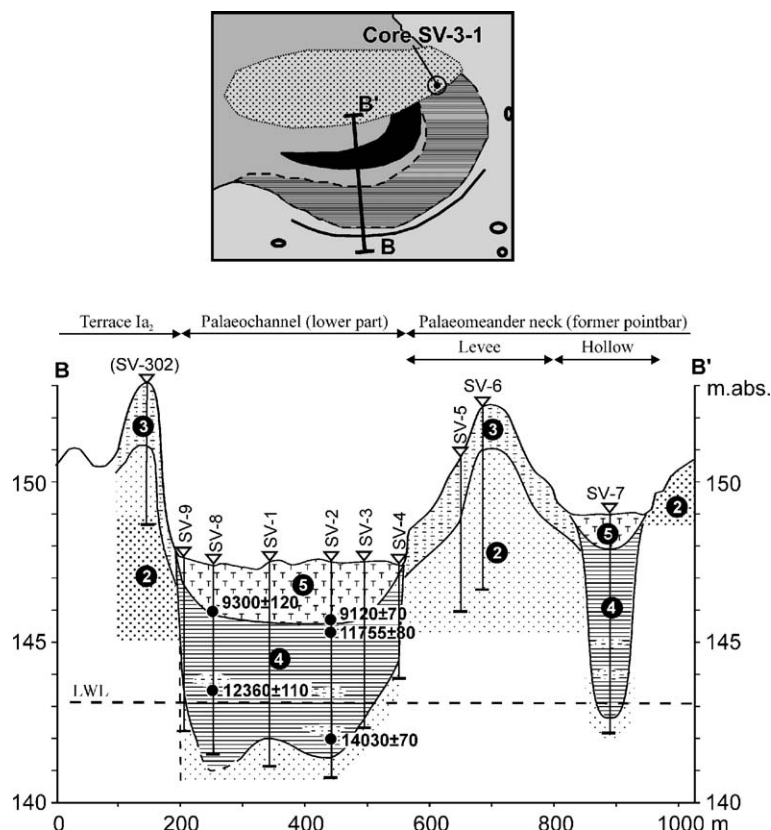


Fig. 6. Geological section across the large meandering channel of the Palaeo-Svapa River near Semenovka village. See location in Fig. 5.

The left side of the palaeochannel cuts Terrace 1, which is 7–10 m above LWL. Its right side is framed by a large levee with a symmetrical profile and the tops 9 m above LWL, that is, roughly even with the surface of Terrace Ia<sub>2</sub>. Coring (cores SV-5, SV-6, Fig. 6) shows a typical sequence of the floodplain sediments: fine- and medium-grained sand with low content of clay (not more than 12%), similar to the channel alluvium found in the palaeochannel trough, and is covered by a layer of sandy loam and silt flood sediments 1.5–2.0 m thick. This levee was formed along the concave bank of the palaeochannel. Its similarity in height with the surface of the left-bank Terrace Ia<sub>2</sub> indicates that the latter was inundated during the floods at the time of the levee formation, thus being a floodplain. The difference in elevation between the Late Valdai palaeochannel bed and floodplain surface is 10–12 m.

### 5.3. River development in the Holocene

Though the Holocene ox-bows vary greatly in size, it is obvious that by the onset of the Holocene channel dimensions had decreased considerably (Fig. 7). The smallest meanders, indicating very low discharges, are characteristic for the Preboreal. One of these ox-bows was abandoned before 9.8 Kyr B.P. Larger ox-bows are dated 8.9 Kyr B.P. Nevertheless, the beginning of the Boreal was marked by a rather dry climate indicated by activation of aeolian processes. Aeolian dunes cover the upper part of the large palaeochannel near Semenovka. Samples of the oxbow lake clays, collected by coring from the depths of 0.6–0.8 and 0.2–0.4 m below the base of aeolian sand, have the radiocarbon age of  $9630 \pm 75$  (Ki-7007) and  $9070 \pm 80$  (Ki-7006) years B.P., respectively. An extrapolated age of the beginning of aeolian sand accumulation is approximately 8700 years B.P.

In the middle Subatlantic a distinct phase of flood decrease is indicated by formation of a well-developed soil on the floodplain. Its presence evidences that the floodplain was not inundated or occasional episodes of flooding were very short. The soil is buried by a layer of laminated overbank deposits 0.5 m thick, which indicates a revival of flooding. This happened after 1.1 Kyr B.P., based on the

radiocarbon dating of charcoal particles at the very top of the buried soil ( $1100 \pm 65$ , Ki-7005).

## 6. Palaeodischarge estimations based on palaeochannel morphology

### 6.1. Application of the hydraulic method to the geological cross-sections

The cross-section of the large palaeochannel of the Svapa River revealed by coring was used for the palaeohydrological estimates with the hydraulic method. This cross-section is located at the palaeochannel riffle, so that it was not subjected to the backwater effects. At the Svapa River the slope of the terrace surface along the palaeochannel axis is 6.5 cm/km. This value can be used as the water slope for approximate palaeohydrological calculations. The water discharges in palaeochannels were calculated using Chezy formula (1) for different water stages. The bed of the palaeochannel was reconstructed at the boundary between channel alluvial sands and oxbow lake clays formed after an active stream abandoned the channel about 14 K years B.P. The maximum flood water level was calculated from the presumption of the floodplain stability during the floods. This presumption is based on a very sharp (goose-neck) shape of the palaeochannel meander with a very narrow meander neck, which was not broken through by the flood flow during the meander evolution. Assuming that the sand with the median grain size of 0.25 mm on the floodplain surface was not eroded during the floods, the critical velocity of erosion initiation was calculated as 0.4 m/s. This velocity corresponds to the maximum floodplain inundation of about 0.7 m. The Manning roughness coefficient was estimated for the river-analogues at 0.024. The calculation shows that at the time of the large palaeochannel abandonment the flood discharge at the mouth of the Svapa River (the basin area of 6310 km<sup>2</sup>) reached  $6400 \text{ m}^3 \text{ s}^{-1}$ . The reconstructed value is close to the mean maximum discharge ( $7500 \text{ m}^3 \text{ s}^{-1}$ ) of the Dnepr River near Kiev (the basin area of 378,000 km<sup>2</sup>).

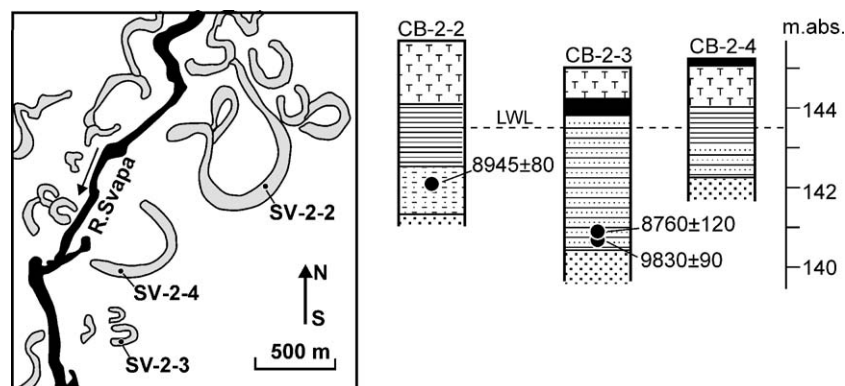


Fig. 7. Holocene ox-bows on the Svapa River floodplain. See Fig. 5 for location and Fig. 4 for legend.

## 6.2. Application of the regime approach based on palaeochannel geometry

Regime formulas (2)–(4) were used to calculate the mean and mean maximum discharges of the active Palaeo-Svapa and Palaeo-Seim rivers. Basin areas were taken from State Hydrological Survey handbooks, and coefficient  $a$  used from hydrological analogues. Palaeochannel width was calculated as an average of two estimates: the mean width of palaeochannels, measured at the crosses on the aircraft and space images  $W_{\text{mean}}$ , and the one-tenth of the mean palaeochannel wavelength  $W_{\text{wl}}$ :

$$W = \frac{W_{\text{mean}} + W_{\text{wl}}}{2} \quad (5)$$

One-tenth of meander wavelength is a well-known ratio for the channel width (Leopold and Wolman, 1957) and is typical for the rivers in the Russian Plain (Popov, 1969). The error of the estimate of width was estimated at about  $\pm 10\%$  (Sidorchuk and Borisova, 2000), therefore the reconstructed width of the Palaeo-Seim River is  $450 \pm 45$  m and that of the Palaeo-Svapa River is  $250 \pm 25$  m.

According to the principle of palaeogeographical analogy, the coefficient  $a$  in formula (4) has to be estimated from the modern region-analogue of the palaeolandscape with large rivers. From the radiocarbon dating we know that the large palaeomeander was abandoned about 14 Kyr B.P. All abandoned palaeomeanders of the Seim and Svapa Rivers are well developed, some of them have very sharp “goose-neck” shapes. Estimates show (Sidorchuk and Borisova, 2000) that one or two thousand years are necessary for such a meander to develop. Therefore the period of active large rivers in the southern Russian Plain should have started about 15–16 Kyr B.P., at the very beginning of the deglaciation. The landscape at that time was of the periglacial steppe type with deep permafrost (Velichko, 2002). Its closest modern hydrological analogue can be found in tundra regions of European Russia and West Siberia, where coefficient  $a$  varies within the range 2.0–2.5 (Sidorchuk et al., 2001b). The rivers in tundra are characterised by short and high spring flood with the runoff coefficient close to 0.9 and by a long period of low flow in nearly empty large channels. Calculations with formula (2)–(4) show the annual and mean flood discharges for the Palaeo-Seim River  $175 \pm 50$  and  $2440 \pm 230 \text{ m}^3 \text{ s}^{-1}$ . For the Palaeo-Svapa River these values are  $85 \pm 20$  and  $1250 \pm 50 \text{ m}^3 \text{ s}^{-1}$ , respectively. This gives an estimate of annual runoff at 420 mm with the range 320–520 mm and annual precipitation 500 mm with the range 375–625 mm.

## 7. Palaeogeographical conditions of river development since the Late Pleniglacial

To reconstruct the main climatic indexes in the Seim River basin the method based on the composition of fossil

floras derived from palynological data was employed. Palynologically studied fluvial sediments fill a segment of a large meander on the Svapa River floodplain (core SV-8). Sediments are represented by alternating layers of sand, clay, and peat with a total thickness of 6 m (Fig. 8). According to radiocarbon dating, these sediments were accumulated during the final part of the Late Weichselian (Late Valdai) glacial epoch, from the Oldest to the Younger Dryas, and during the entire Holocene, which amounts approximately to 14 thousand years. According to the age–depth model based on the majority of the dates (see Fig. 8), the fastest deposition was characteristic for the grey lake clay with low organic content accumulated in the late glacial time ( $1.0 \text{ mm a}^{-1}$ ). At the beginning of the Holocene the accumulation rate decreased dramatically, with a simultaneous increase in the organic content of the sediments. During the Preboreal and Boreal periods of the Holocene a 20 cm layer of black clay was formed with the rate of  $0.09 \text{ mm a}^{-1}$ . Since the beginning of the Atlantic, peat accumulation has occurred at the site. An apparent peat accumulation rate was the lowest in the early Atlantic ( $0.1 \text{ mm a}^{-1}$ ), reached its maximum during the late Atlantic–early Subboreal ( $0.3 \text{ mm a}^{-1}$ ), and decreased again after the late Subboreal ( $0.24 \text{ mm a}^{-1}$ ). The actual slowing down of the peat growth must have been even greater, considering a decrease in post-sedimentation compression and decomposition of the peat towards the surface. Detailed palynological analysis permitted use of the palaeofloristic (“arealogram”) method of reconstruction. The modern region-analogues were located for twelve dated palaeo-floras from core SV-8 and other sections of fluvial deposits in the adjacent parts of the Seim River basin. The present-day climatic and hydrologic conditions in these regions are believed to be close to hydro-climatic characteristics in the Seim River basin at the corresponding time in the past. The accuracy of these reconstructions depends on the accuracy of palaeo-floristic definitions based on detailed pollen analysis, on the richness of the resulting fossil floras, on the accuracy of the data on present-day geographical ranges of plants—components of the fossil floras, on the sizes of the region-analogues, and the variability of hydro-climatic characteristics within them. The accuracy of palynological analysis and the richness of palaeo-flora depend not only on palynologist’s personal experience, but also on the type of sediment, vegetation type, and the degree of pollen preservation. For example, the late glacial floras are relatively poor, so that not all analysed samples provide sufficient data for palaeofloristic reconstruction. The accuracy of the match of geographical position to a modern analogue to a fossil flora depends not only on the richness of the latter, but also on the knowledge of the modern geographical distribution of each plant genus or species. Often the area of a region-analogue remains rather large and includes different types of vegetation associations. Therefore in this study all centres were located on the map (Fig. 10) and additionally checked afterwards against the



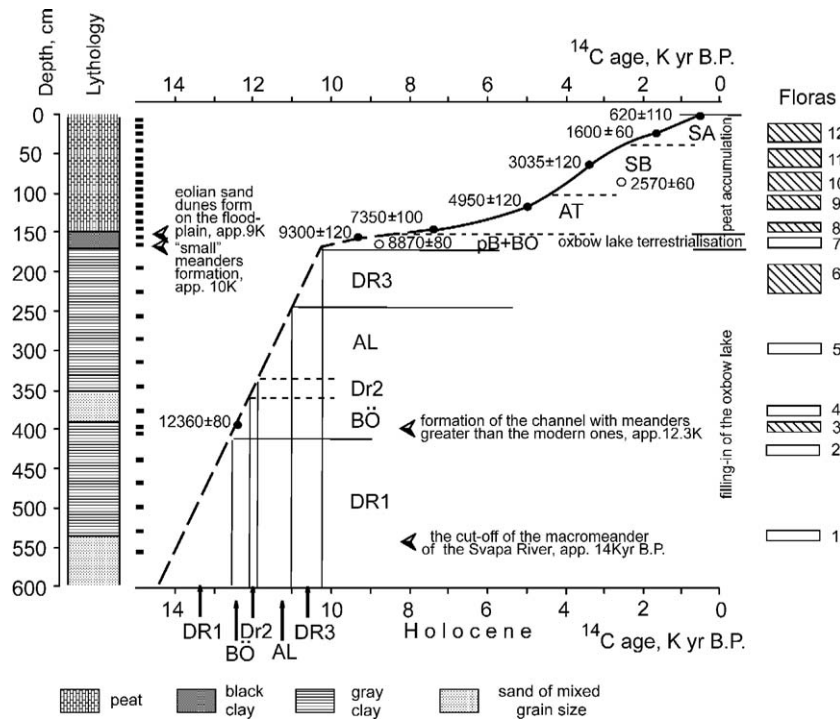


Fig. 8. Sedimentation rates and environmental conditions of the Svapa River palaeochannel infill.

types of plant communities, reconstructed from the pollen assemblage of a given sample. Sometimes such comparison enabled us to reduce the area of the region-analogue, but even then the resulting areas remained large enough to show a substantial variability of hydro-climatic characteristics within them. The reconstructed ranges of the climatic parameters are shown in Fig. 11 along with the mean values as the shaded boxes, their vertical size corresponding to the time intervals characterised by each fossil flora.

### 7.1. The late glacial landscape

In the late glacial part of the pollen record from section SV-8 (LPAZ 1–3) the content of arboreal pollen (AP) varies from 20% to 40%. Scots pine (*Pinus sylvestris*) is predominant among the forest-forming trees (Fig. 9a). In some intervals, pollen of tree birch (*Betula alba*) is also abundant, spruce (*Picea abies*) being the third important component of woodlands. Nevertheless, the landscape role of pine, birch, and spruce communities remained minor even during the warm interstadial phases, as indicated by the high proportion of non-arboreal pollen (NAP) in the spectra, by the presence of heliophytes (especially light-demanding plants), such as *Helianthemum* spp., as well as by the abundance and diversity of meadow and steppe herbaceous plants (Varia) (Fig. 9b).

In this part of the profile, pollen of trees and shrubs were typical of those growing at present in the regions with a highly continental climate, mainly in Siberia (e.g., *Pinus sibirica*, *Abies sibirica*, *Larix* sp., *Alnaster fruticosus*). According to V.P. Grichuk (1969), such species were

typical of the ‘glacial’ floras in the Russian Plain. Another characteristic feature of glacial floras is the presence of xerophytes (*Ephedra* spp., *Eurotia ceratoides*, *Kochia prostrata*, etc.) resistant to cold winters. The finds of pollen and spores of cold-tolerant plants, such as shrub alder (*A. fruticosus*), a typical Arctic-montane species, *Selaginella selaginoides*, and *Botrychium boreale*, growing at present in the European and West-Siberian tundra, strongly suggest existence of permafrost in the late glacial time. Based on these data, one can conclude that during the Late Glacial the vegetation in the region belonged to the periglacial forest steppe type. It combined open woodland, cold steppe, and meadow communities with some tundra elements.

In LPAZ 1, generally corresponding to the Oldest Dryas, AP is dominated by Scots pine (c. 80%). According to the studies of recent pollen spectra (Pyavchenko, 1966; Levkovskaya, 1973), it is strongly over-represented in the forest tundra, where the actual landscape role of pine woodlands is very low. The remaining 20% of tree pollen are made up equally by spruce and birch. Pollen of Siberian pine forms a continuous curve in zone 1. Changes in the AP composition in LPAZ 1 suggest warmer summer conditions in the later part of the Oldest Dryas.

The percentages of NAP rise from app. 50% to almost 90% within LPAZ 1, largely due to a sharp increase in Cyperaceae pollen contents. The latter probably indicates local high ground moisture, possibly due to a spread of permafrost with a relatively thin active layer. Presence of xerophytes (*Ephedra* sp., *Kochia scoparia*) and cryophytes (*B. boreale*, *Saxifraga* spp.) among the herbaceous plants

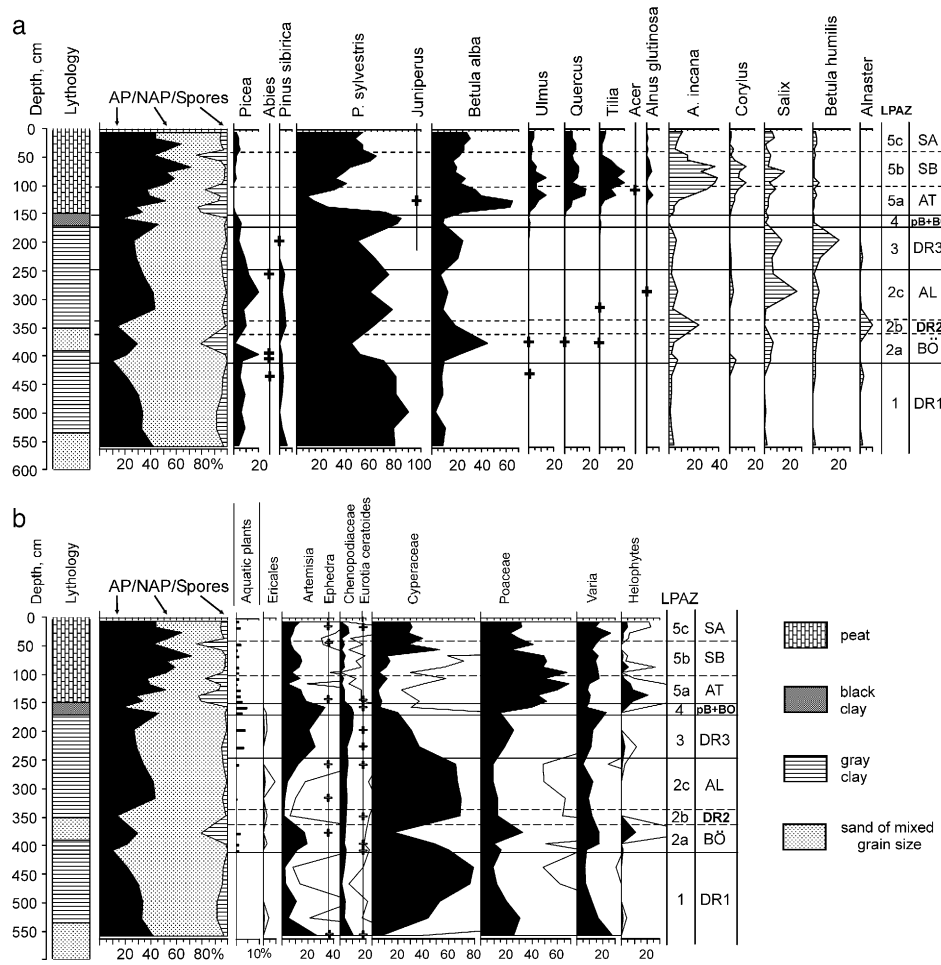


Fig. 9. Pollen diagrams of the Late Valdai palaeochannel infill (core SV-8): (a) composition of arboreal pollen (tree pollen sum=100%); (b) composition of non-arboreal pollen (NAP=100%).

also suggests a greater degree of the continentality of climate compared to the present.

Palynological study of the sediments, corresponding to the initial stage of filling in of the large palaeochannel of the Seim

River (core S-4, 13,800 ± 85 year B.P., Ki-6984), reveals a pollen assemblage generally similar to those at the base of LPAZ 1 in SV-8. The flora of this sample (FI-1 in Fig. 10) characteristically combines cryophile (*A. fruticosus*, *S.*

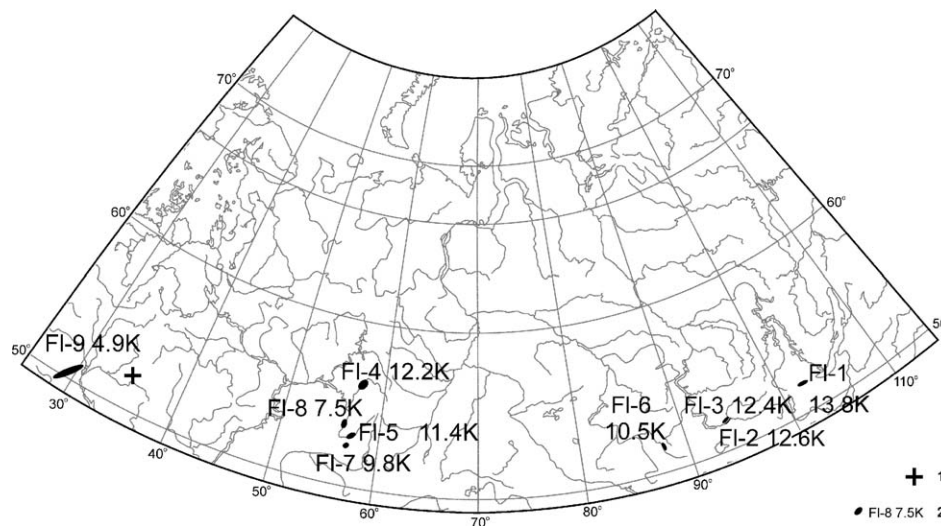


Fig. 10. Location of the modern region-analogues to the fossil floras from the Seim River basin.

*selaginoides*) and xerophile (*Ephedra* sp.) plants, inhabitants of the boreal forest, steppe, meadow, and riverine communities, as well as heliophytes (*Helianthemum* spp.).

The closest modern floristic analogue for this assemblage can be found in the forest steppe in the middle reaches of the Irkut River basin, west of the Lake Baikal and north of the East Sayan Mountains (Fig. 10). Within this small area, larch and pine forest grow next to south Siberian meadow steppes, with patches of spruce forest in the river valleys. The area is characterised by a cold semi-arid and extremely continental climate. The mean January temperature is  $-24^{\circ}\text{C}$  and that of July is about  $16^{\circ}\text{C}$ . The mean annual precipitation varies between 425 and 475 mm. The mean annual surface runoff depth is 300 mm. The region is situated near the boundary of the permafrost zone with high annual runoff coefficient close to 0.67. Another sample of the fluvial deposits filling in the large palaeochannel of the Seim River was obtained from the basal part of core S-7 taken in the same profile as core S-4 (Fig. 3). According to the radiocarbon date ( $12,630 \pm 70$  year B.P., Ki-6985), it corresponds to the final part of the Oldest Dryas, and therefore to the upper part of LPAZ 1 in SV-8 section. Pollen assemblage of this sample is similar to those in the upper part of zone 1. The flora of this sample (Fl-2 in Fig. 10) is distinctive for the diversity of xerophytes and xerohalophytes, which suggest a rapid drying of the topsoil in the watershed areas in relatively warm summers. Similar conditions occur at the present time in southern Siberia. A region-analogue for fossil flora 2 lies at the headwaters of the Yenisey River, within an inter-mountain depression downstream from the confluence of the Biy-Khem and Kakhem rivers (Fig. 10). In this area south Siberian grass dry steppes are found next to mountain forest of *P. sibirica* and *Larix sibirica*. The area is characterized by extremely cold winters with the mean January air temperature from  $-23$  to  $-27^{\circ}\text{C}$ , while the summer is warm, the mean July temperature being about  $18^{\circ}\text{C}$ . The annual magnitude of air temperature changes is about  $43^{\circ}$ , and that is  $15^{\circ}$  greater than at the study site at the present time. The mean annual temperature is minus  $4^{\circ}\text{C}$ , providing favourable conditions for the spread of permafrost. Therefore the runoff coefficient could be even higher, than at the previous region-analogue and is taken equal to 0.75. The mean annual precipitation is app. 400 mm and calculated runoff depth is about 300 mm.

LPAZ 2 in profile SV-1–8 corresponds to the Bølling-Allerød interstadial warming with a short intermittent cooling known as the Older Dryas in the European biostratigraphy. The zone is characterized by an increase in AP contents, as well as that of spores in sub-zone 2a (Fig. 9a). In sub-zone 2a, pollen curve of *B. alba* rises considerably, along with the increase in pollen contents of the mesophile shrubs: *Alnus incana*, *Salix*, and *Betula humilis*. These changes indicate an increase in precipitation at that period. The corresponding peak of *Artemisia* pollen within NAP group can be explained by a high proportion of species growing on eroded and sandy ground in this genus, rather than by the expansion of the dry

steppe communities, as this local maximum of *Artemisia* coincides with the increase in the contents of spores (mainly those of Polypodiaceae ferns), pollen of hygrophytes, such as *Sparganium* and *Typha latifolia*, and aquatic plants (Fig. 9b).

Flora 3 derived from a dated sample at the depth of 3.9–4.0 m in sub-zone 2a ( $12,360 \pm 110$  years B.P., Ki-6999) belongs to the beginning of the Bølling Interstadial. It includes inhabitants of various forest biotopes—dark coniferous taiga forest (*P. abies*, *A. sibirica*, *P. sibirica*), light coniferous and mixed boreal forest (*P. sylvestris*, *Pteridium aquilinum*, *B. alba*), along with species of riverine shrub associations, heaths, meadows, and psammophytes (e.g., *Spergula*). The presence of some xerophytes in this flora indicates that the periglacial steppe coenoses were preserved at that time in favourable conditions, although their landscape role decreased compare to the Oldest Dryas. A region-analogue for fossil flora 3 also lies at the headwaters of the Yenisey River. It is shifted to the north with respect to the region-analogue 2 (Fig. 10). In this area south Siberian grass dry steppes are also the main vegetation type, though the role of dark coniferous mountain forest of *Picea*, *P. sibirica* and *A. sibirica* there is slightly greater compared to region-analogue 2. The region is characterized by milder climatic conditions with the mean January air temperature  $-23^{\circ}$  and that of July about  $17^{\circ}\text{C}$ , which is similar to the reconstruction based on fossil flora 1. Therefore, the runoff coefficient could be the same as at the first region-analogue (0.67). The mean annual precipitation is app. 450 mm, and the calculated runoff depth is about 300 mm.

In the upper part of sub-zone 2a rare pollen grains of the broad-leaved deciduous trees (*Quercus*, *Ulmus*, and *Tilia cordata*) were found. In spite of their low pollen values, these trees might actually occur at the site, as confirmed by generally mesophile character of the pollen assemblage and by presence of pollen of other relatively heat-demanding plants, such as *Nymphaea alba*. In the end of the Bølling the area was covered by a complex vegetation of the forest steppe type, where birch and pine copses with minor participation of lime, oak, and elm were the most common type of woody vegetation. The presence of the broad-leaved trees in the region implies a complete degradation of permafrost at this period.

Similar palynological data were obtained for the fluvial deposits infilling the palaeochannel of the second generation in the Seim River valley. Flora 4, derived from a dated sample at the depth of 3.0–3.1 m in the borehole S-11 (see Fig. 4, date  $12,250 \pm 70$  year B.P., Ki-6987), also includes the broad-leaved cool-temperate tree species, as well as *Alnus glutinosa*—tree alder, growing on the waterlogged ground. A diversity of the hygro- and hydrophytes in this flora and an absence of xerohalophytes in its composition suggest an increase in the rainfall, being in good agreement with the reconstruction based on the correspondent part of SV-8 pollen profile. A region-analogue for fossil flora 4 lies at the headwaters of the Ufa River at the Southern Ural



Mountains (Fig. 10). In this region, meadow steppes come into close contact with southern Urals pine and birch forests and spruce-fir sub-taiga forests with minor presence of the broad-leaved trees. The area is characterized by significantly milder climatic conditions compared to the region-analogues 2 and 3: the mean January air temperature there is  $-16^{\circ}\text{C}$  and the mean July temperature is about  $17^{\circ}\text{C}$ . The mean annual precipitation is 650 mm, and the runoff depth is about 200 mm with 70% of the flow passing during the spring flood. Annual runoff coefficient is 0.31, and that for the flood period is about 0.6. The present-day conditions in the region-analogue indicate that already in the late Bølling the mean annual air temperature in the Seim River basin was above freezing, which permitted the relatively thermophile broad-leaved trees to penetrate into this area from their glacial refuges.

The Older Dryas cold stage is poorly represented in SV-8 pollen diagram, where sub-zone 2b is tentatively correlated to this time interval. In the composition of pollen spectra this cooling is reflected by the increased NAP content and by the peaks in *Alnaster* and *A. incana* pollen curves.

Sub-zone 2c is distinctive for the highest AP percentages for the entire Late Glacial (up to 45% of the total terrestrial pollen and spores) and for the highest spruce pollen content in this profile (c. 20% of tree pollen sum). The Allerød was, therefore, the most favourable time for the expansion of dark coniferous forest of *P. abies* and *P. sibirica* in this region. *Abies* also took part in these communities in the end of this interval. Of the mesophile broad-leaved species registered in sub-zone 2a, *Tilia* and *Corylus* persisted in the Allerød. The presence of *A. glutinosa*, a peak of *Salix* pollen curve and an abundance of sedges within NAP group point to a relatively high precipitation during this period.

A dated sample from section S-11 (see Fig. 4, 11,450 ± 60 year B.P., Ki-6986) corresponding to sub-zone 2c in SV-8 profile has a similar pollen assemblage, except for a lower content of Cyperaceae pollen. Instead, it features a greater abundance and diversity of the helophytes—plants, growing on wet meadows, near the water margin, and in shallow water (*Sparganium* spp., *Menyanthes trifoliata*, *Sagittaria sagittifolia*, and others) (Fl-5 in Fig. 10). Tree pollen is strongly dominated by birch, though the actual presence of Scots pine at the site is confirmed by the finds of pine *stomata*. Rare pollen grains of *Larix* indicate that larch participated in the pine forest at this period. Of the relatively thermophile trees and shrubs, pollen of *Ulmus*, *Tilia*, *Corylus*, and *Viburnum* is registered. A modern analogue for fossil flora 5 is located at the headwaters of the Belaya River near the Southern Urals (Fig. 10). The region is currently occupied by forest steppe, where meadow steppes are associated with birch and aspen woods and grow next to larch-pine open forests with steppe elements in the herbaceous cover, and to the broad-leaved (oak-linden) forests of Southern Ural type. This area is characterized by the mildest climatic conditions for the entire Late Glacial,

with the mean January air temperature  $-16^{\circ}$  and that of July  $18^{\circ}\text{C}$ . The mean annual precipitation there reaches 700 mm, the runoff depth is about 225 mm, with 60% of the flow passing during the spring flood. Annual runoff coefficient is 0.32, and that for the flood period is about 0.56.

LPAZ 3 correlated to the Younger Dryas is distinguished for a new rise of NAP curve, as well as for a distinct maximum of *Artemisia* pollen and a smaller peak of Chenopodiaceae inside the NAP group. *P. sylvestris* and *B. alba* dominate AP. Of the dark coniferous trees, only *P. abies* persists through zone 3, its pollen curve showing a gradual decline towards the top of the zone. Rare pollen grains of Siberian pine are registered in this zone. Of the cold-tolerant shrubs, *B. humilis* is the most abundant, and *Alnaster* is present. Relatively thermophile trees once again disappear from the local flora (Fl-6, Fig. 10). Changes in the pollen assemblages and the flora are indicative of both colder and more arid climatic conditions compared to the previous interval, with probable re-establishment of permafrost in the region. A region-analogue for fossil flora 6 is situated in the middle reaches of the Biya River in the northern Altai Mountains (Fig. 10). In the vegetation cover of this area, open larch woodlands with steppe elements in the ground cover and patches of steppes are spread next to fir and Siberian pine forests on the mountain slopes. Birch and Scots pine communities occur on sandy soil. The area is characterized by a severe, continental and relatively dry climate with the mean annual precipitation of 450 mm and the runoff depth 225 mm, with a rather high annual runoff coefficient (0.5). The mean January air temperature is  $-18^{\circ}\text{C}$ , and that of July  $15^{\circ}\text{C}$ . These values suggest that in the Younger Dryas the mean annual air temperature in the Seim River basin once again dropped below freezing, which implies a possibility of re-establishment of permafrost during this cold stage.

## 7.2. The Holocene landscapes

LPAZ 4 corresponds to the layer of dense black clay with high organic content, which represents the final stage of infilling of the oxbow lake, formed in the fragment of the Svapa River palaeochannel, with the lacustrine sediments. According to the age–depth curve (Fig. 8), this layer corresponds to the Preboreal and Boreal periods of the Holocene. At this stage the accumulation rate became extremely low ( $0.1\text{ mm a}^{-1}$ ), and an increasingly shallow lake was gradually overgrown by vegetation. Composition of the pollen spectra indicates that the climatic conditions at this time were both warm and dry: NAP contents reached their maximum values for the entire profile (c. 60% of the total terrestrial pollen and spores), *Artemisia* and Chenopodiaceae being the most abundant within the NAP group. AP group was strongly dominated by *P. sylvestris*, with all mesophile arboreal species at their minimum values. Thermophile trees, such as elm and lime, re-appeared in the area. An abundance of pollen of the sub-aquatic and

aquatic plants (*Myriophyllum* spp., *Lemna*, *Potamogeton*) in zone 4 is typical for a shallow stagnant fresh-water lake with peaty shores.

A similar pollen assemblage was found in the radiocarbon-dated layer of black clay at the depth of 4.35–4.45 m in section SV-2–3 (see Fig. 7, 9830±70 year B.P., Ki-7004) in the ox-bow of the Svapa River (“small meanders”). Flora of this sample features a variety of xerophytes and plants growing on barren ground with discontinuous vegetation cover, thus indicating arid conditions in the Preboreal. It coincides well with the formation of a new generation of palaeochannels with relatively small meanders in the Seim River basin and a subsequent development of aeolian sand dunes (c. 9 Kyr B.P.) on the floodplains in the area. The region-analogue for fossil flora 7 lies between the headwaters of the rivers Belaya and Ural (Fl-7 in Fig. 10), near the boundary between the forest steppe (meadow steppe of the Volga-Kazakhstan type with birch copses) and the herb-grass steppe. Forests formed by pine and broad-leaved species occur along the eastern margin of this region. The area is characterized by relatively warm and dry climatic conditions: the mean January temperature is –15.5°C, with July being 19°C. The mean annual precipitation is 550 mm, while the runoff depth is only 125 mm, annual runoff coefficient being as low as 0.23.

LPAZ 5 corresponds to the layer of peat in section SV-1–8 and includes the remaining part of the Holocene. Peat initiation was probably connected with the increase in precipitation compared to the Boreal. In the pollen diagram, the Atlantic (sub-zone 5a) is characterised by a rapid rise of AP content (Fig. 9a). Tree pollen is dominated by birch in the lower part of the sub-zone, with the increasing proportion of the broad-leaved tree pollen (first *Ulmus* and *Quercus*, and later *Tilia*). High percentages of Polypodiaceae spores, very typical of the initial stages of peat accumulation, are registered in the basal part of sub-zone 5a. Among NAP, Poaceae become dominant, along with the diverse wetland plants (Fig. 9b). Flora 8 derived from the dated peat sample at the depth of 1.4–1.5 m (SV-8, 7350±100 year B.P., GIN-11952) includes also some xerophytes (*E. ceratoides*, *K. scoparia*, and *Ephedra distachya*), which indicates that the degree of continentality of climate was still relatively high in the Early Atlantic. A region-analogue for fossil flora 8 is located at the headwaters of the Belaya River in the Southern Ural Mountains (Fig. 10). Meadow steppes (forest steppe) of the Volga-Ural type, true herb-grass steppes of the Volga-Kazakhstan type, and broad-leaved forests occupy the area at present. The mean January air temperature for this region is –15.5°C, and the mean July temperature is 18.5°C. The mean annual precipitation is 670 mm there, and runoff depth is about 160 mm with 68% of flow passing during the spring flood. The annual runoff coefficient is 0.24, and that for the period of flood is about 0.5.

Very similar palynological data were obtained for the basal layer of peat from section S-6 at the large palae-

ochannel of the Seim River, confirming that the peat initiation had a regional (probably, climatic) rather than local cause.

Pollen contents of the broad-leaved trees and of the mesophile shrubs, especially those of *A. incana* and *Corylus avellana*, grew rapidly towards the end of the Atlantic, pointing to the progressive warming accompanied by a diminishing continentality of climate. The AP sum reaches app. 60% of the spectra. The warmest conditions were achieved in the late Atlantic, as is evidenced by the presence of *Acer tataricum* and *Ulmus campestris* pollen at the depth of 1.0–1.2 m (SV-8, 4900±120, GIN-11425). Rare pollen grains of *Carpinus* were also registered in this layer. Although possibly still wind-blown from some distance, this pollen indicates the time when the most oceanic climatic conditions existed at the site, promoting the maximum spread of *Carpinus betulus* to the east. Flora 9, derived from this layer, contains many mesophile plants, both arboreal and herbaceous. A region-analogue for fossil flora 9 lies between the middle reaches of the Dnepr and South Bug rivers (Fig. 10). Within this area, meadow steppes of the East European type (oak forest steppe) grow next to pine-oak and oak forests with other broad-leaved species. The region is characterized by mild climatic conditions with the mean January air temperature –6° and the mean July temperature 18.5°C. Mean annual precipitation is 650 mm, runoff depth is as low as 90 mm, with annual runoff coefficient 0.14. Based on this reconstruction, the late Atlantic can be considered a “climatic optimum” of the Holocene, when the warmest and the most oceanic climatic conditions were achieved in this region. The warming was especially well expressed in the changes of winter (mean January) temperatures, which is typical of the interglacial epochs in the East-European Plain in general (Velichko et al., 2004).

During the Subboreal (sub-zone 5b) AP contents reached their maximum values (c. 70%) for the entire profile. Along with a gradual decline of *Betula*, *Ulmus*, *Quercus*, and then *Tilia* and mesophile shrubs, *Pinus* content increases once again, and *Picea* pollen appears in the spectra after a break in the Atlantic. These changes probably reflect some cooling along with the increase in the continentality of climate. The most warmth-loving species disappear from the local flora, while the apparent peat accumulation rate increases slightly, possibly due to slower decomposition of the organic remains.

Flora 10, which characterizes the earlier part of the Subboreal (estimated age c. 4 Kyr B.P.), is close to that of the late Atlantic, except for being slightly poorer. It is possible that rare pollen grains of spruce found at the base of sub-zone 5b were transported by wind from some distance. Nevertheless, their presence indicates a southward advance of spruce, probably in response to the winter cooling. At present, the range of *P. abies* is roughly limited from the south by the Seim river valley in its lower reaches and by the Svapa River valley. Increase in the continentality of climate and decrease in the rainfall may also explain the

raise of *Artemisia* pollen contents in the lower part of sub-zone 5b.

In the end of the Subboreal AP again became dominated by Scots pine. Of the broad-leaved deciduous trees, only *Quercus robur* remained a relatively important forest-forming species. Pollen spectra became similar to the modern ones, with slightly lower proportions of *Ulmus* and *Tilia* pollen. The southern boundary of spruce range must have passed then near the study-site, as it does at present, as *Picea* pollen constantly occurs in the upper part of sub-zone 5b, and such a typical associate of spruce communities as a club-moss *Lycopodium annotinum* is registered at this level. Fossil flora 11 of the late Subboreal, with very few exceptions, do not contain species alien to the contemporary flora of the studied area. Using the floristic region-analogue method it is possible to outline a relatively broad area, which includes the study site. In such cases the deviations of the main climatic indexes from the previous or subsequent time-slice are deduced on the basis of the changes in pollen assemblages, reflecting the changes in vegetation patterns rather than in the composition of fossil floras.

This is also true for the flora of early Subatlantic. At this period pollen content of elm and lime rise a little compared to their minimum values at the Subboreal/Subatlantic boundary (sub-zone 5c). Along with the further rise of *Picea* curve and abundance of Cyperaceae and meadow plants among NAP, these changes imply a slight decrease in the continentality of climate with respect to the Subboreal. On the whole, both the vegetation and climate in the Subatlantic became very similar to the present. The latest part of the Subatlantic (app. 600 years) is not represented in section SV-1–8, as the top layer of peat was destroyed by excavation.

## 8. Discussion

Morphological, geological, geochronological and palynological information for the Seim River basin enables reconstruction of the landscape, climate and hydrological history of this region (Fig. 11). The amount of the available palaeogeographical data on different time-intervals varies, influencing the reliability of the suggested interpretations.

The weakest evidence relates to the hydrological regimen at the time of Terrace 1 formation. This terrace consisting of one or two levels is widely represented in the southern Russian Plain river valleys. Palaeolithic humans settled on its surface 12–22K years B.P. (Velichko et al., 1997). The terrace is composed of more than 15–20m of medium- and fine-grain horizontal and cross-bedded sand, often covered by laminated loam. The general longitudinal slope of the terrace surface is lower than that of the modern rivers: at the Seim and Svapa confluence it is about 3 cm/km. The fluvial features on the terrace surface are very unclear and cannot be used to define the channel pattern. Based on these scarce data we can assume that Terrace 1 was formed at the Last

Glacial Maximum or somewhat earlier by shallow flows overloaded with sand.

Extraordinary morphological features—large meandering palaeochannels, mark the next hydrological period. In the Seim River basin their width and meander wavelength are ten to fifteen times greater than those of the modern channels with the same drainage area. Large channels were entirely different in their hydraulic geometry from the channels of the previous stage, which formed Terrace 1. Their longitudinal slopes are twice as steep as those of the channels of the previous generation. Therefore the Palaeo-Svapa River flooded Terrace 1 during the large channel period, while the channel of Palaeo-Seim was incised into the same terrace.

Using a straightforward morphological approach with the general regime formulas, one could reconstruct annual discharges of such large rivers at 20–80 times of the modern values (see Dury, 1965). Such enormous surface runoff estimations would lead to equally improbable estimates of precipitation and cause an understandable disbelief in palaeohydrological reconstructions. According to the principle of palaeogeographical analogue, the hydraulic and regime formulas (1)–(4) should be calibrated using the closest modern hydrological region-analogue of a palaeolandscape (Sidorchuk and Borisova, 2000). With this evident improvement the morphological approach provides the means for reliable hydrological and climatic reconstructions. The closest hydrological analogue of the Seim River basin for the Late Glacial is an open tundra landscape with permafrost, incised gullies, long severe winters with considerable snowfall, short and high spring floods, mainly concentrated within a channel, and nearly empty river channels during the rest of the year. In such a landscape, the annual water losses to evatranspiration and infiltration are low, and runoff coefficients can be close to 0.8–0.9. The channels in such an environment are disproportionately wide compared to the water flow during most of the year, with large meanders, formed by high flood discharges. At the same time, the total amount of annual precipitation and surface runoff can be rather low because of high efficiency of river channel erosion. Using such an analogue, the annual precipitation for the period of large channel formation in the Seim River basin can be reconstructed at about 500mm (close to the contemporary level), and the annual surface runoff at about 420mm (three to four times the modern one due to much lower losses) (Fig. 11).

The accuracy of these estimates is not high—about  $\pm 20\%$ . River channel morphology is characterised by significant inertia, so that the sizes of alluvial relief forms of the lowland sandy rivers do not change much due to the short-term (several decades) oscillations of river flow. A measurable transformation of the channel width and meander wavelength usually takes hundreds of years. Accuracy of the reconstruction of palaeochannel geometry is low, and the modern analogues are never exact. Therefore,



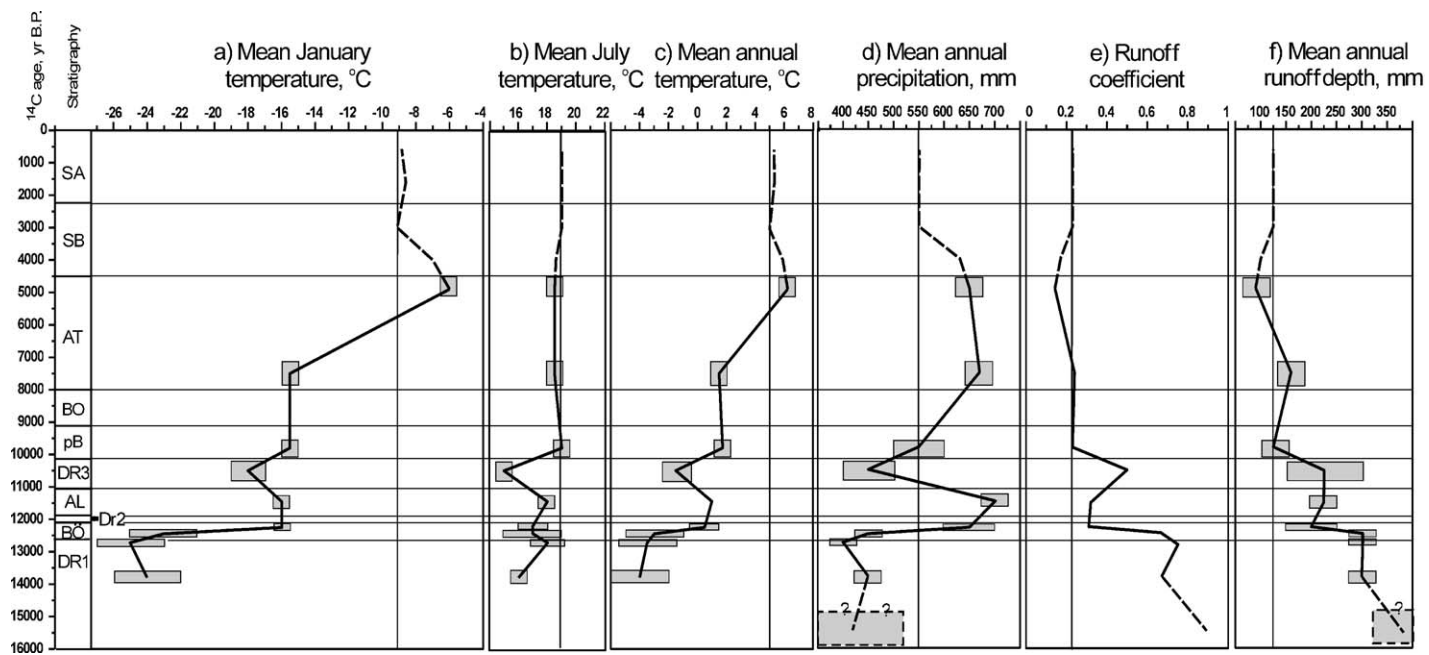


Fig. 11. Reconstructed hydro-climatic changes in the Seim River basin during the Late Glacial and the Holocene.

palaeohydrological reconstructions using palaeochannel morphology can reveal only long-term changes of a relatively high magnitude.

Another problem, related to the large palaeochannels, is the reliability of their age estimation. Fluvial deposits of these channels are usually very poor in organic matter, and nearly forestless environment of the period of their formation makes finds of fossil wood in channel alluvium rare. AMS dating based on microscopic organic remnants in such deposits is rather uncertain due to a high probability of re-deposition of the dated material from older sediments. Therefore most of the age estimates for the large palaeochannels in the Russian Plain were based on  $^{14}\text{C}$  dates obtained from the basal layers of their infill (Sidorchuk et al., 2001a), rich enough with organic matter for conventional radiocarbon dating (see Sidorchuk et al., 2001b). For the large palaeochannels of the Seim and Svapa Rivers the oldest dates based on such infilling deposits (supposedly corresponding to the end of the active transformations of the large channels) are  $13,800 \pm 85$  years B.P. (Ki-6984) in the Palaeo-Seim;  $13,510 \pm 85$  years B.P. (Ki-6991) in the Palaeo-Prutishche, and  $14,030 \pm 70$  years B.P. (Ki-6997) in the Palaeo-Svapa. Well-developed shapes of the large meanders prove that they evolved during a relatively long period. The model of meander transformation suggests that at least for 1–2 thousand years they should have developed in the frozen deposits (Sidorchuk and Borisova, 2000). The most probable time boundaries for the period of an active large river in the Seim River basin are from 16 to 14K radiocarbon years B.P. (app. between 19 and 17K calibrated years ago).

The period of non-steady decrease of surface runoff continued from the Oldest Dryas to the Preboreal. During this period the large meanders were abandoned and smaller channels formed, as reflected both in the floodplain and channel morphology, as well as in the lithological sequences and the history of flora and vegetation. The changes in geographical position (see Fig. 10) and hydro-climatic characteristics of the palaeofloristic region-analogues (Fig. 11) reflect an overall trend from more to less continental conditions and complexity of climate change during the Late Glacial. This trend is most clearly expressed in the general rise of the winter air temperatures from minus  $24\text{--}25^\circ\text{C}$  in Oldest Dryas to minus  $17^\circ\text{C}$  at the Holocene boundary. Secondary oscillations can be seen on this general trend. Air temperature was lowest in the late part of the Oldest Dryas and in the Younger Dryas. The warm intervals correspond to the early part of the Oldest Dryas, Bølling, and Allerød. Negative mean annual air temperatures clearly indicate the periods of permafrost existence during the Oldest Dryas–early Bølling and in the Younger Dryas.

Precipitation changes in the Late Glacial generally followed temperature changes, the cold stages being relatively dry, and the warm stages relatively humid, with the maximum of precipitation achieved in the Bølling–Allerød Interstade. The surface runoff is not directly

connected with annual precipitation as the water losses depend on air temperature. Runoff coefficient is inversely correlated with the temperature changes showing a strong overall decrease during the Late Glacial. Generally following changes in the runoff coefficient, the surface runoff also decreased considerably during this period (Fig. 11). This general tendency is expressed in palaeochannel morphology. The width and meander wave length of the paleochannels decreased from the macromeanders of the first generation, to secondary meandering channels still larger than the modern ones, and finally to small Preboreal ox-bows preserved on the contemporary floodplain with the sizes smaller than those of the modern meanders. Palaeochannels with the largest meanders were formed during the driest stage of all (Fig. 11). This seemingly paradox situation is explained by the lowest water losses during the cold climate with the permafrost.

More short-term interrelations between precipitation changes and water losses led to secondary variations in the surface runoff. For example, during the warm Bølling–Allerød interval an increase in precipitation caused a moderate increase in surface runoff, so that the surface runoff during the warm and humid Allerød Interstadial was approximately equal to that during the cold and dry Younger Dryas.

The last stage of the relative stability of the hydrological regimen with small variation of water runoff in the modern rivers includes the entire Holocene (Fig. 11). The sizes of the ox-bows on the modern floodplain, as well as the sizes of the meanders of the modern channels vary across a broad range, but do not show any temporal regularity. Their differences remain within a general range of the river channel variability, caused by the hydraulics of channel flow, by bank sediments and by a complicated interaction of the in-channel and floodplain hydrology. Palynological estimates show an air temperature increase from early to late Atlantic. Precipitation increased significantly from the Preboreal to the early Atlantic, with a very low increase in runoff. Surface runoff slightly decreased during the Atlantic. Palaeo-floristic reconstruction shows a similarity between the late Atlantic and early Sub-Boreal, while the younger floras (and, therefore, hydro-climatic conditions) did not differ much from the modern one. Variations in the composition of vegetation reflect only minor temperature changes around contemporary values. However, buried soil evidence indicates some decrease in the floodplain inundation about 1.1K years B.P. and an increase in the sedimentation on the floodplain during the last millennium.

## 9. Conclusion

In the general sequence of the Late Quaternary hydrological events four periods can be distinguished: 1) A period of sandy Terrace 1 formation tentatively

correlated to the Last Glacial Maximum. The terrace was formed by shallow flows overloaded with sand and modified by cryogenic and aeolian processes. 2) A period of large meandering rivers formation with very high surface runoff 16–14 Kyr B.P. Large meandering palaeochannels developed in cold and continental climate with precipitation close to or lower than modern and a very high runoff coefficient caused by continuous spread of permafrost. 3) A period of non-steady decrease of surface runoff with large meander abandonment and smaller channel formation 14–9 Kyr B.P. Against the overall trend towards warming during the Late Glacial, expressed primarily in the rise of winter temperatures, secondary climatic oscillations are distinguished. The intervals with the lowest air temperatures (the Oldest and Younger Dryas) were favourable for permafrost development, providing high runoff coefficients and therefore increasing the runoff depth even in spite of a decrease in precipitation. 4) A period of relative stability of hydrological regimen and small variation of water runoff in modern-type rivers (9K year B.P.–present). The highest air temperature was achieved in the late Atlantic, while both the precipitation and the runoff reached their maximum values for the entire Holocene in the early Atlantic. According to the palaeohydrological and palynological data, the climate close to modern occurred in the region since the late Subboreal.

### Acknowledgements

Authors are grateful to S. Baslerov, Yu. Kononenko, D. Lizunkov, and E. Sheremetskaya for their assistance in the field works. Financial support of this work was received from the Russian Foundation of Basic Research (RFBR), Projects No. 97-05-64708 and 00-05-64021.

### References

- Davis, W.M. 1896. The Seine, the Meuse and the Mosell. *Geographic Magazine*, VII: 189–202, 228–238.
- Dury, G.H., 1958. Tests of a general theory of misfit streams. *Inst. British Geographers Trans. Papers Pub.*, vol. 25, pp. 105–118.
- Dury, G.H., 1964a. Principles of underfit streams. *Professional Paper - Geological Survey (U.S.)* 452-A.
- Dury, G.H., 1964b. Subsurface exploration and chronology of underfit streams. *Professional Paper - Geological Survey (U.S.)* 452-B.
- Dury, G.H., 1965. Theoretical implications of underfit streams. *Professional Paper - Geological Survey (U.S.)* 452-C.
- Evstigneev, V.M., 1990. *Rechnoy Stok i Gydrologicheskiye Raschety*. Moscow Univ. Press, Moscow (in Russian).
- Gregory, K.J., 1996. Introduction. In: Branson, J., Brown, A.G., Gregory, K.J. (Eds.), *Global Continental Changes: The Context of Palaeohydrology*, Special Publication No. 115. Geological Society, London, pp. 1–8.
- Grichuk, V.P., 1969. Glyatsial'nye flory i ikh klassifikatsiya. In: Gerasimov, I.P. (Ed.), *Posledniy Lednikovyi Pokrov na Severo-Zapade Evropeiskoy Chasti SSSR*. Nauka, Moscow, pp. 57–70 (in Russian).
- Grimm, E.C., 1987. CONISS: a FORTRAN 77 program for stratigraphically constrained cluster analysis by the method of incremental sum of squares. *Computers and Geosciences* 13, 13–35.
- Grimm, E.C., 1990. TILIA and TILIA\*GRAPH.PC spreadsheet and graphics software for pollen data. *INQUA, Working Group on Data-Handling Methods. Newsletter* 4, 5–7.
- Khotinsky, N.A., 1977. *Golotsen Severnoy Evrazii*. Nauka, Moscow (in Russian).
- Khrutskiy, S.V., 1983. Geologicheskoye stroenie i rel'ef. In: Mil'kov, F.N. (Ed.), *Poseymye. Voronezh University press, Voronezh*, pp. 13–19 (in Russian).
- Leopold, L.B., Miller, J.P., 1954. Postglacial chronology for alluvial valleys in Wyoming. *United States Geological Survey Water Supply Papers* 1261, 61–85.
- Leopold, L.B., Wolman, M.G., 1957. River channel pattern: braided, meandering and straight. *Professional Paper - Geological Survey (U.S.)* 282-B.
- Levkovskaya, G.M., 1973. Zonal'nye osobennosti sovremennoi rastitel'nosti i retsentnykh sporovo-pyl'tsevykh spektrov Zapadnoi Sibiri. In: M.I. Neustadt (Editor-en-chief), *Metodicheskiye Voprosy Palinologii*. Nauka, Moscow, pp. 116–120 (in Russian).
- Makkaveev, N.I., 1955. *Ruslo Reki i Erosiya v Eye Basseine*. USSR Academy of Sciences Press, Moscow (in Russian).
- Panin, A.V., Sidorchuk, A.Yu., Chernov, A.V., 1999. Historical background to floodplain morphology: examples from the East European Plain. In: Marriott, S.B., Alexander, J. (Eds.), *Floodplains: Interdisciplinary Approaches*, Special Publication No. 163. Geological Society, London, pp. 217–229.
- Panin, A.V., Sidorchuk, A.Yu., Baslerov, S.V., Borisova, O.K., Kovalukh, N.N., Sheremetskaya, E.D., 2001. Osnovnyye etapy istorii rechykh dolin tsentra Russkoy ravniny v pozdnem Valdae i Golotsene: rezul'taty issledovaniy v srednem techenii reki Seim. *Geomorfologiya* 2, 19–34 (in Russian).
- Popov, I.V., 1969. Deformatsii rechykh rusel i gidrotekhnicheskoye stroitel'stvo. *Gidrometeoizdat, Leningrad* (in Russian).
- Pyavchenko, N.I., 1966. Rezul'taty palinologicheskogo izucheniya torfyanikov Yeniseiskoi polosy Sibiri. *Znacheniyeye Palinologicheskogo Analiza dlya Stratigrafii i Paleofloristiki*. Nauka, Moscow, pp. 232–238 (in Russian).
- Rotnicki, K., Borowka, R., 1985. Definition of subfossil meandering palaeochannels. *Earth Surface Processes and Landforms* 10, 215–225.
- Sidorchuk, A.Yu., 1975. Osnovnyye etapy evolutsii del'ty Yany. In: Ivlev, A. (Ed.), *Geomorfologiya i Paleogeografiya Dal'nego Vostoka*. Geographical Society, Khabarovsk, pp. 116–180 (in Russian).
- Sidorchuk, A., 1996. Gully erosion and thermoerosion on the Yamal Peninsula. In: Slaymaker, O. (Ed.), *Geomorphic Hazards*. Wiley, Chichester, pp. 153–168.
- Sidorchuk, A.Yu., 2003. Floodplain sedimentation: inherited memories. *Global and Planetary Change* 39 (1–2), 13–29.
- Sidorchuk, A.Yu., Borisova, O.K., 2000. Method of palaeogeographical analogues in palaeohydrological reconstructions. *Quaternary International* 72 (1), 95–106.
- Sidorchuk, A., Borisova, O., Panin, A., 2001a. Fluvial response to the late Valdai/Holocene environmental change on the East European Plain. *Global and Planetary Change* 28, 303–318.
- Sidorchuk, A., Borisova, O., Kovalukh, N., Panin, A., 2001b. Lateglacial and Holocene palaeohydrology of the lower Vychegda river, western Russia. In: Maddy, D., Macklin, M.G., Woodward, J.C. (Eds.), *River Basin Sediment Systems: Archives of Environmental Change*. A.A. Balkema Publishers, pp. 265–296.
- Velichko, A.A. (Ed.), 2002. *Dinamika landshaftnykh komponentov i vnutrennikh morskikh basseynov Severnoy Evrazii za posledniye 130000 let*. GEOS, Moscow (in Russian).
- Velichko, A.A., Grekhova, L.V., Gribchenko, Yu.N., Kurenkova, E.I., 1997. *Pervobytniy Chelovek v Extremal'nykh Usloviyakh Sredy: Stoyanka Eliseevichi*. Institute of Geography Russian Academy of Sciences, Moscow (in Russian).



- Velichko, A.A., Pisareva, V.V., Faustova, M.A., 2001. Podkhody k rekonstruktsii oledeneniya srednego pleistotsena. In: Velichko, A.A., Shik, S.M. (Eds.), *Oledeneniya Srednego Pleistotsena Vostochnoy Evropy*. GEOS, Moscow, pp. 143–149 (in Russian).
- Velichko, A.A., Zelikson, E.M., Borisova, O.K., Gribchenko, Yu.N., Morozova, T.D., Nechaev, V.P., 2004. Kolichestvennyye rekonstruktsii klimata Vostochno-Evropeskoy ravniny za poslednie 450 tysyach let. *Izvestiya AN, Ser. Geogr.*, vol. 1, pp. 1–19 (in Russian).
- Volkov, I.A., 1960. O nedavnem proshlom rek Ishim i Nura. *Trudy Laboratorii Aerometodov AN SSSR* 9, 15–19 (in Russian).
- Volkov, I.A., 1962. K istorii rechnykh dolin yuga Zapadno-Sibirskoy nizmennosti. *Trudy Instituta Geologii i Geofiziki SO AN SSSR* 27, 34–47 (in Russian).
- Volkov, I.A., 1963. Sledy moschnogo stoka v dolinakh rek yuga Zapadnoy Sibiri. *Doklady AN SSSR* 151 (3), 648–651 (in Russian).
- Wohl, E.E., Georgiadi, A.G., 1994. Holocene palaeomeanders along the Sejm River, Russia. *Zeitschrift für Geomorphologie* 38 (3), 299–309.